BIODIVERSITAS
Volume 26, Number 9, September 2025
Pages: 4396-4411

ISSN: 1412-033X
E-ISSN: 2085-4722
DOI: 10.13057/biodiv/d260913

Sexual dimorphic traits of the head morphology of Chinese edible frog *Hoplobatrachus rugulosus* in Musuan, Philippines

JASMIN S. RIZALDA[1,♥], MARK LLOYD G. DAPAR[1,2,♥♥]

[1]Institute of Biological Sciences, College of Arts and Sciences, Central Mindanao University. University Town Musuan, Maramag, Bukidnon 8710, Philippines. Tel.: +63-8835-61910, ♥email: s.rizalda.jasmin@cmu.edu.ph, ♥♥email: f.marklloyd.dapar@cmu.edu.ph
[2]Microtechnique and Systematics Laboratory, Natural Science Research Center, Central Mindanao University. University Town Musuan, Maramag, Bukidnon 8710, Philippines

Manuscript received: 5 July 2025. Revision accepted: 13 September 2025.

Abstract. *Rizalda JS, Dapar MLG. 2025. Sexual dimorphic traits of the head morphology of Chinese edible frog* Hoplobatrachus rugulosus *in Musuan, Philippines. Biodiversitas 26: 4396-4411.* Sexual dimorphism in amphibians often reflects ecological pressures, reproductive strategies, and behavioral roles. This study investigated sex-based differences in head, snout, and tympanum shapes in *Hoplobatrachus rugulosus* using landmark-based geometric morphometric analysis. A total of 60 adult frogs (30 males, 30 females) were photographed, and 33 head, 7 snout, and 8 tympanum landmarks were digitized. Generalized Procrustes Analysis (GPA) and Relative Warp Analysis were used to assess shape variation. Statistical tests included MANOVA, Discriminant Function Analysis (DFA), and Procrustes distance calculations. Significant shape differences were found between sexes for all traits: head ($p = 1.03 \times 10^{-10}$, $\eta^2 = 0.584$; Procrustes $d^2 = 0.07$), snout ($p = 2.18 \times 10^{-5}$, $\eta^2 = 0.381$; $d^2 = 0.05$), and tympanum ($p = 0.0001$, $\eta^2 = 0.368$; $d^2 = 0.04$). DFA correctly classified 90% of individuals by head shape and 75% by snout and tympanum. Females exhibited broader, more symmetrical heads and snouts, which may support feeding efficiency and fecundity. Males displayed more irregular and asymmetrical snout and tympanum shapes, likely associated with acoustic signaling and mate competition. Fluctuating asymmetry in tympanum shape across both sexes may reflect developmental stress from environmental factors such as agrochemical use or habitat disturbance. Geometric morphometrics effectively revealed subtle shape variation overlooked by traditional methods. However, the approach requires high-quality images, technical expertise, and may not capture behavioral or physiological traits. Future research should incorporate functional data, including bite force and mating acoustics, to better understand the adaptive significance of cranial dimorphism in this species.

Keywords: Anurans, evolution, frog, morphology, sexual dimorphism

INTRODUCTION

Sexual dimorphism, the phenotypic differentiation between males and females, is widespread in amphibians and is primarily shaped by the combined forces of natural and sexual selection (Račković et al. 2019; Fondren 2023). These differences often reflect adaptations linked to ecological roles, reproductive strategies, or behavioral pressures that affect the sexes differently (Schäuble 2004; Dapar et al. 2014; Portik et al. 2019). Common dimorphic traits include variation in body size, cranial shape, limb proportions, and sensory organs, all of which may contribute to reproductive fitness and survival (Portik et al. 2019).

In anurans, sexual dimorphism frequently manifests as female-biased size dimorphism (SSD), where larger female body size is typically associated with fecundity advantages, such as greater egg production and reproductive output (Silva et al. 2020; Vági et al. 2020). Males, on the other hand, may exhibit traits that enhance mating success, including enlarged forelimbs for amplexus, vocal sacs, and tympana optimized for acoustic signaling (Tsuji and Matsui 2001; Juarez et al. 2023). The direction and extent of dimorphism are often influenced by ecological variables such as altitude, temperature, and habitat structure, as well as by mating systems and competition intensity (Petrović et al. 2017; Caldart et al. 2019; Pincheira-Donoso et al. 2021). While head shape can contribute to feeding efficiency or call production, evidence of dietary overlap between sexes in many frog species suggests these differences may be more closely tied to reproduction than to ecological divergence (Lin and Ji 2005; Chen et al. 2023). Additionally, asymmetries in traits such as the tympanum have been linked to developmental instability and may reflect individual fitness or environmental stressors (Bosch and Márquez 2000).

The Chinese edible frog *Hoplobatrachus rugulosus* (Wiegmann, 1834), which is native to Southeast and East Asia (including China, Thailand, Vietnam, Laos, Cambodia, and Myanmar), has been introduced and is considered an invasive species in the Philippines (Diesmos et al. 2008). Its presence in these ecosystems raises biosecurity concerns, particularly due to the potential for competition with native amphibians, disease transmission, and disruption of local ecological balances (Lin et al. 2023). The *H. rugulosus* displays sexual dimorphism primarily in body size and certain cranial traits. Females are generally larger and have longer heads and hind limbs, whereas males tend to have proportionally larger eyes, longer forelimbs, and larger tympana (Lin and Ji 2005). This species breeds during the rainy season from April to August, during which males produce courtship calls using paired vocal sacs to attract

females and compete with rival males (Wei et al. 2014; Traijitt 2020). Although these vocalizations enhance reproductive success, they also increase the risk of predation, illustrating a reproductive trade-off that may drive the evolution of sexually dimorphic acoustic and cranial traits (Yang et al. 2022; Juarez et al. 2023).

Morphometric analysis has long been used to quantify body shape and size in amphibians and remains a cornerstone of taxonomic and ecological research (Kaliontzopoulou 2011). Traditional morphometrics relies on linear measurements, ratios, and angles, but these approaches may overlook subtle shape differences that are biologically relevant (Dapar et al. 2015). Geometric morphometrics, by contrast, uses anatomical landmarks to assess shape variation while preserving spatial relationships, allowing for more accurate and detailed comparisons of morphology between groups (Kaliontzopoulou 2011; Ilić et al. 2019). Recent applications of geometric morphometrics in anurans have examined sexual dimorphism in species such as *Aparasphenodon brunoi*, *Anaxyrus americanus* (Murta-Fonseca et al. 2020; Üzüm et al. 2021; Fondren 2023; Tokita et al. 2023). However, in *H. rugulosus*, most studies have used only traditional morphometric approaches. As a result, there remains a lack of high-resolution analysis of cranial shape differences between sexes in this species, particularly regarding snout and tympanum morphology.

This study aims to fill that gap by using landmark-based geometric morphometrics to evaluate sex-based shape differences in the head, snout, and tympanum of *H. rugulosus*. Specifically, the objectives are to (i) compare head morphometrics between males and females, (ii) assess the statistical significance of any observed differences, and (iii) explore their possible biological and ecological implications. We hypothesize that *H. rugulosus* exhibits significant sexual dimorphism in cranial shape, with females showing broader head and snout morphology consistent with fecundity-driven selection, and males displaying more irregular tympana and snouts that may reflect adaptations to acoustic communication and mating competition.

MATERIALS AND METHODS

Place and duration of the study

The study was conducted at Central Mindanao University, Musuan, Maramag, Bukidnon, Philippines (Figure 1: Coordinates: 7.8592° N, 125.0515° E). The surrounding area includes academic buildings and residential houses, also present in the area are man-made ponds, rice fields, and small creeks that provide suitable aquatic and semi-aquatic habitats for frogs. Opportunistic sampling was carried out over a 19-day period, from March 21 to April 8, 2025. Nocturnal sampling was conducted from 18:00-22:00 (Solania and Fernandez-Gamalinda 2018). A total of 60 adult *Hoplobatrachus rugulosus* were collected, consisting of 30 males and 30 females. The sample size was determined based on comparable studies on sexual dimorphism in anurans (Murta-Fonseca et al. 2020) and other taxa such as fish (Solis et al. 2015; Cabuga et al. 2025). No DENR gratuitous permit was required, as the species collected are classified as invasive alien species. Although no formal collection or handling permits were necessary, all procedures adhered to ethical standards for the humane use of animals in scientific research. All procedures followed ethical standards for animal research and complied with IACUC guidelines. Individuals were handled with care to minimize stress, and only non-invasive morphometric measurements were taken. Upon completion of data collection, specimens were released at their original capture locations.

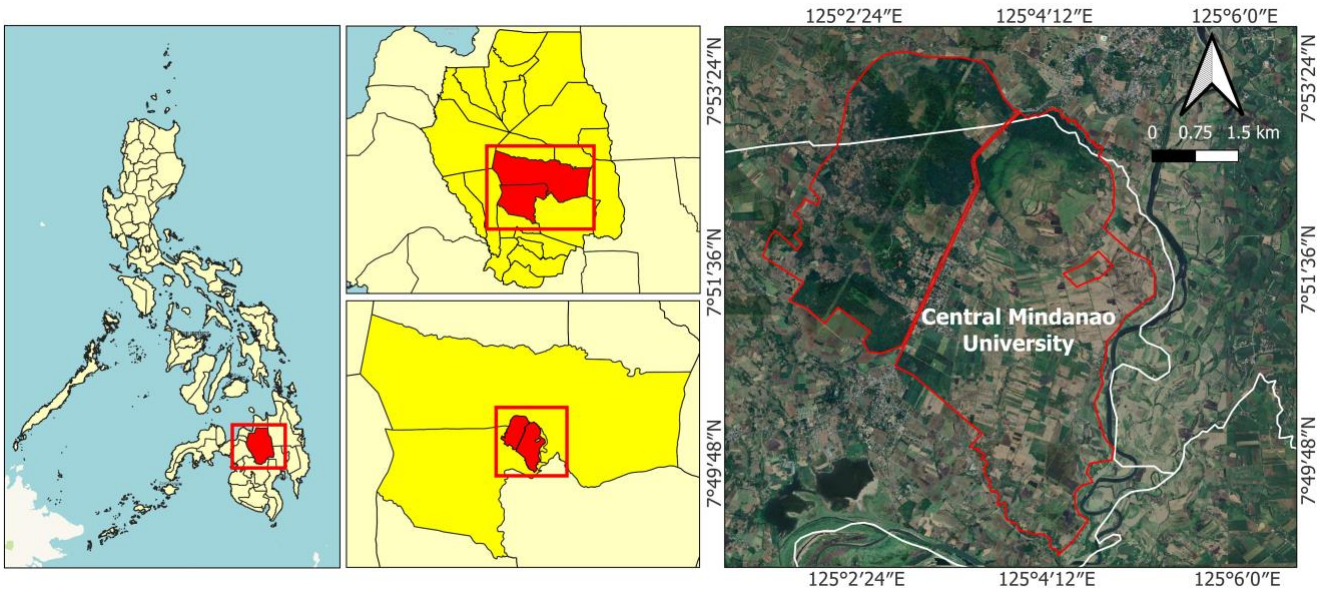

Figure 1. Map of the Central Mindanao University, Philippines

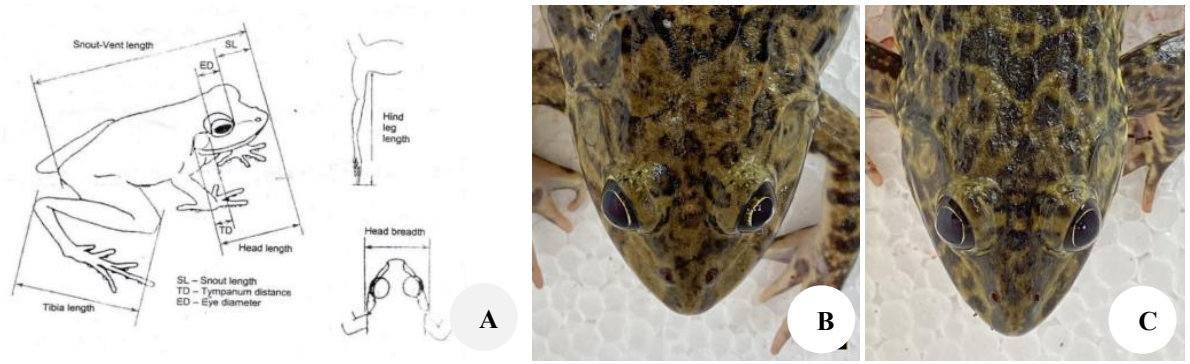

Figure 2. A. Morphometric measurements based on Haribon Foundation Guidelines for Amphibians and Reptiles Survey (2004), B. Female (F04), C. Male (M03)

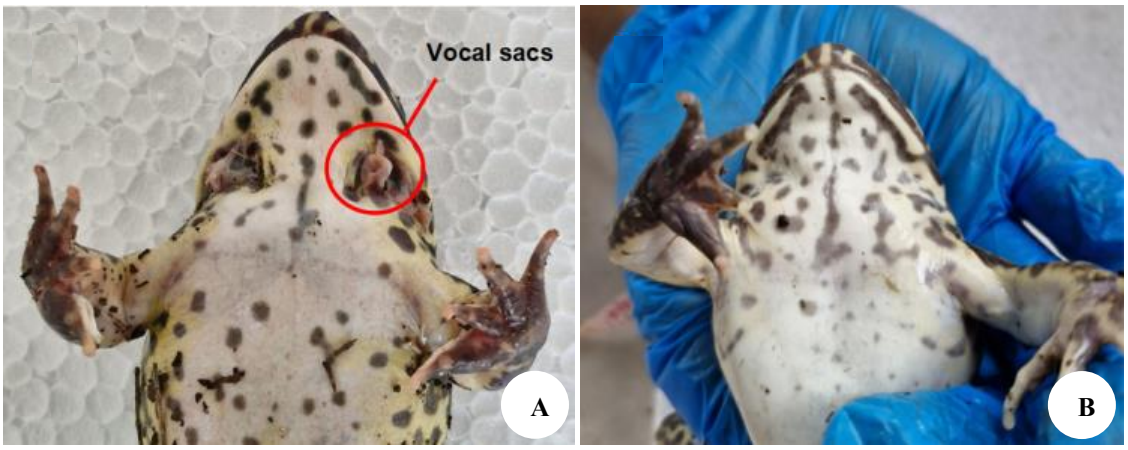

Figure 3. Sex differentiation in *Hoplobatrachus rugulosus*. A. Male (M01), B. Female (F01)

Sampling techniques

Various microhabitats of anurans were surveyed, including creeks, ponds, and rice paddies (Delima et al. 2006; Nuñeza et al. 2017). All individuals encountered along transects were captured and placed in a clean polyethylene plastic bag (Flores et al. 2024). Moreover, the image acquisition and morphometric measurements were conducted the following morning.

Species identification and sex determination

For species identification, taxonomic references and illustrated keys were used to confirm the species. Morphometric measurements of each individual were taken using a digital caliper, measured in millimeters (mm), including: (i) Snout Vent Length (SVL), (ii) Head Length (HL), and (iii) Head Breadth (HB) following the Haribon Foundation Guidelines for Amphibians and Reptiles Survey (2004) (Figure 2). The average adult Snout-Vent Length (SVL) is 99.4 mm in males and 117.3 mm in females (Rongchapho et al. 2021). To ensure all specimens were adults, only individuals exceeding the established SVL thresholds for maturity were included: ≥75 mm SVL for females and ≥60 mm SVL for males, based on criteria from Lin and Ji (2005). Juvenile frogs falling below these thresholds were excluded from the analysis. Moreover, the phenotypic sex of each individual was determined by examining secondary sexual characteristics. These characteristics included the presence of vocal sacs (Figure 3), the presence or absence of nuptial pads, position in amplexus, and whether individuals produced release calls when held (Fondren 2023).

Image acquisition and geometric morphometric analysis

Digital photographs (jpeg) of the dorsal head of each specimen were taken (Murta-Fonseca et al. 2020). A mini studio was constructed using styrofoam, maintaining a fixed camera-to-subject distance of approximately 25 cm. All images were captured using an iPhone 11 (12 MP, 326 PPI) under consistent natural morning light between 8:00 and 10:00 AM. To reduce motion blur, live frogs were photographed only after they had naturally calmed down. While no artificial lighting was used, care was taken to maintain uniform lighting conditions across all samples. A total of 33 landmarks were used for head shape analysis, including 7 for the snout and 8 for the tympanum region. These landmarks were placed along key anatomical features such as the eyes, snout, jawline, cranial crests, tympanum, and orbital ridges (Figure 4, Table 1). The selection of landmark points in the head, snout, and tympanum of *H. rugulosus* was modified from the landmarks of Murta-

Fonseca et al. (2020) and Fondren (2023). Currently, there are no existing studies that provide a standardized set of landmarks specifically for *H. rugulosus.* Therefore, the landmarks were adapted to suit the morphological features of this species.

Geometric morphometric analysis was performed to process the images. The software used in this study was Thin plate spline Utility (TpsUtil), Thin plate spline Digitization (TpsDig), Thin plate Spline (TpsSpline), and Thin plate spline Relative Warps (TpsRelW). The images were imported into TpsUtil to create a TPS file. The generated TPS files were converted to digital format, and landmarks homologous to those of the *H. rugulosus* were manually placed using TpsDig ver. 2.32. Relative warps and Procrustes distances were then generated. Moreover, Generalized Procrustes Analysis (GPA) was performed in TpsRelW to remove non-shape variation due to size, position, and orientation. Lastly, the generation of relative warps and Procrustes distance was performed using Thin plate spline Relative Warps (TpsRelW) and Thin plate Spline (TpsSpline), respectively.

Table 1. List of landmarks used for geometric morphometric analysis of *Hoplobatrachus rugulosus*

Head	Snout	Tympanum
Posterior most corner of the left eye	Posterior point of the left snout	Right midpoint of the left tympanum
Right midpoint of the left tympanum	Midpoint of the left snout	Posterior most point of the left tympanum
Posterior most point of the left tympanum	Anterior point of the left snout	Left midpoint of the left tympanum
Left midpoint of the left tympanum	Anterior midpoint of the snout	Anterior most point of left tympanum
Anterior most point of left tympanum	Anterior point of the right snout	Anterior most point of the right tympanum
Posterior left of the maxilla	Midpoint of the right snout	Right midpoint of the right tympanum
Midpoint of the left maxilla	Posterior point of the right snout	Posterior most point of the right tympanum
Posterior point of the left snout		Left midpoint of the right tympanum
Midpoint of the left snout		
Anterior point of the left snout		
Anterior midpoint of the snout		
Anterior point of the right snout		
Midpoint of the right snout		
Posterior point of the right snout		
Midpoint of the right maxilla		
Posterior right of the maxilla		
Anterior most point of the right tympanum		
Right midpoint of the right tympanum		
Posterior most point of the right tympanum		
Left midpoint of the right tympanum		
Posterior most corner of the right eye		
Posterior of the right eye		
Posterior point of the right orbital crest		
Right midpoint of the right eye		
Anterior point of right the orbital crest		
Anterior most corner of the right eye		
Center of the right nostril		
Center of the left nostril		
Anterior most corner of the left eye		
Anterior point of the left orbital crest		
Left midpoint of the left eye		
Posterior point of the left orbital crest		
Posterior of the left eye		

Figure 4. Actual photo of Chinese edible frog (*Hoplobatrachus rugulosus*) with 33 landmarks (Head), 7 landmarks (Snout), and 8 landmarks (Tympanum)

Statistical analysis

All statistical procedures were done using Paleontological Statistics (PAST) software version 5.1 (Hammer et al. 2001). PAST software was used to perform Principal Component Analysis (PCA) to visualize head morphology differences between female and male *H. rugulosus*, Discriminant Function Analysis (DFA) to classify each specimen into female and male based on their differences in head morphology, and Multivariate Analysis of Variance (MANOVA) to test if sexes are significantly different in terms of head morphology in the species. Lastly, univariate comparisons of Snout-Vent Length (SVL), Head Length (HL), and Head Breadth (HB) between sexes were analyzed using independent t-tests. A significance threshold of $p<0.05$ was used for all tests. Furthermore, to support interpretation, data visualization included histograms, box plots, heat maps, and deformation grids, which highlighted patterns of sexual dimorphism in cranial morphology.

RESULTS AND DISCUSSION

Validation of sex identification

Prior to morphometric analysis, sex identification of *H. rugulosus* was validated using diagnostic morphological traits. Females were generally larger in body size, while males were characterized by the presence of vocal sacs, nuptial pads, and comparatively smaller body size. This confirmation ensured that the male and female groups analyzed represented biologically distinct categories.

Geometric morphometric analysis

A total of 30 female and 30 male individuals were used to assess variation in head, snout, and tympanum shapes. A total of 33, 7, and 8 landmarks were used to identify variations of the head, snout, and tympanum shapes, respectively. The relative warps were selected based on a >5% variance threshold, supported by scree plot inspection to ensure inclusion of components with meaningful shape variation. Moreover, the shape variations were summarized using histograms, box plots, heat maps, and relative warp analysis.

Shape variations

Geometric morphometric analysis of *H. rugulosus* revealed that the majority of shape variation was captured by the first few Relative Warps (RWs) across different head regions. For overall head shape, RW1 accounted for 44.69% of the total variation, followed by RW2 (14.11%) and RW3 (10.43%). In the snout shape, the first four RWs explained most of the variation, with RW1 contributing 48.76%, RW2 at 31.98%, RW3 at 9.10%, and RW4 at 6.14%. Tympanum shape variation was described by the first five RWs, with RW1 explaining 29.89%, RW2 at 19.20%, RW3 at 12.54%, RW4 at 10.97%, and RW5 at 7.50% (Table 2).

Head shape variations

Results showed that the distributions of RW1, RW2, and RW3 scores were approximately normal, indicating that most individuals cluster near the mean for each relative warp (Figure 8). The boxplots reveal consistent patterns of sexual dimorphism in head shape: females tend to lean toward the positive extremes in RW1 and RW2, and toward the negative extreme in RW3, whereas males exhibit the opposite trends (Figure 9).

Discriminant Function Analysis (DFA) showed 90% of *H. rugulosus* that were correctly classified into their respective groups, indicating strong morphological differentiation (Figure 10). The difference in overall head shape of *H. rugulosus* between sexes is further justified by the visible pattern of variation differentiating the sexes, with a Procrustes distance of 0.07 (Figure 11). This result is further supported by MANOVA (Table 3), where the p-value of 1.034E-10 indicates a significant difference in head shape. Therefore, the results suggest that sex influences the variation in head shape of *H. rugulus.*

Snout shape variations

Results showed that the distributions of RW1 to RW4 scores were approximately normal, indicating that individuals generally cluster near the mean for each relative warp (Figure 8). The boxplots reveal distinct sexual dimorphism in snout shape: females tend to lean toward the opposing extremes in RW1, RW2, and RW4, and toward the positive extreme in RW3, while males exhibit the opposite trends (Figure 9).

Discriminant Function Analysis (DFA) showed 75% of *H. rugulosus* that were correctly classified into their respective groups, indicating strong morphological differentiation (Figure 10). The sexual dimorphism in the snout shape of *H. rugulosus* is further supported by the visual pattern differentiating the sexes with a procrustes distance of $d^2 = 0.05$ (Figure 11). This result is further supported by MANOVA (Table 3), where the p-value of 2.177E-05 indicates a significant difference in snout shape.

Tympanum shape variations

Results indicates that the distributions of RW1 to RW5 scores are approximately normal, with most individuals clustering near the mean (Figure 8). The boxplots reveal consistent patterns of sexual dimorphism in tympanum shape: females generally lean toward the negative extreme in RW1, RW3, RW4, and RW5, while males lean toward the positive extremes in these same RWs. In RW2, the pattern is reversed, with females leaning toward the positive extreme and males toward the negative (Figure 9).

Discriminant Function Analysis (DFA) showed 75% of *H. rugulosus* that were correctly classified into their respective groups, indicating strong morphological differentiation (Figure 10). The sexual dimorphism in the tympanum shape of *H. rugulosus* is further justified by the visible pattern of the tympanum shape variation differentiating the sexes with a procrustes distance of $d^2 = 0.04$ (Figure 11). This result was further supported by MANOVA (Table 3), which showed a significant difference of 0.0001159 indicating a significant difference in tympanum shape.

Moreover, the value of head parameters and the summary of morphology between male and female *H. rugulosus* in terms of head, snout, and tympanum shapes is shown in Table 5.

Table 2. Variation in the head, snout, and tympanum shapes of *Hoplobatrachus rugulosus* as explained by each of the significant relative warps and their corresponding percentage variance

		Negative extreme	Positive extreme
Head	RW1 (44.69%)	The variation is characterized by the constriction of right points from anterior to tympanum. There is also an expansion on the left and right orbital crest. Moreover, moderate expansion on the posterior left maxilla and left eyes	The variation is characterized by the constriction of left points from the anterior to tympanum. There is also an expansion on the posterior right maxilla and moderate expansion on the right tympanum as well
	RW2 (14.11%)	The variation is characterized by the constriction of the left and right posterior points in the tympanum and orbital crest. There is also an expansion on the snout specifically on the right anterior and midpoint of the snout	The variation is characterized by the constriction of the left and right anterior snout. There is also expansion on the left and right posterior eyes and orbital crest as well
	RW3 (10.43%)	The variation is characterized by the constriction of the right of anterior snout up to the anterior point of tympanum. There is also an expansion of the posterior left maxilla and the left tympanum	The variation is characterized by the constriction of left tympanum and left and right orbital crest. There is also an expansion of the posterior right maxilla and in the posterior tympanum
Snout	RW1 (48.76%)	The variation is characterized by the constriction of the left and right anterior and midpoint snout. There is also an expansion on the left and right posterior maxilla	The variation is characterized by the constriction left and right posterior maxilla. There is also an expansion on the left and right anterior and midpoint snout
	RW2 (31.98%)	The variation is characterized by the constriction left and right posterior maxilla. There is also an expansion on the left and right anterior and midpoint snout	The variation is characterized by the constriction left and right midpoint to posterior maxilla. There is also an expansion on the left and right anterior snout and midpoint of rostrum
	RW3 (9.10%)	The variation is characterized by the constriction of the left and right anterior and midpoint snout. There is also an expansion on the left and right posterior maxilla	The variation is characterized by the constriction left and right posterior maxilla. There is also an expansion on the left and right anterior and midpoint snout
	RW4 (6.14%)	The variation is characterized by the constriction of the left and right anterior and midpoint snout. There is also an expansion on the left and right posterior maxilla	The variation is characterized by the constriction left and right posterior maxilla. There is also an expansion on the left and right anterior and midpoint snout
Tympanum	RW1 (29.89%)	The variation is characterized by the constriction of the left tympanum. While the expansion on the right tympanum	The variation is characterized by the constriction right tympanum. While the expansion is on the left tympanum
	RW2 (19.20%)	The variation is characterized by the constriction right tympanum. While the expansion is on the left tympanum	The variation is characterized by the constriction of left midpoint to posterior of right tympanum and left and right midpoint to posterior left tympanum. While the expansion is on the anterior to right midpoint of right tympanum and anterior to left and right midpoint of left tympanum
	RW3 (12.54%)	The variation is characterized by the constriction left tympanum. While the expansion is on the right tympanum	The variation is characterized by the constriction left tympanum and anterior to left and right midpoint of right tympanum. While the expansion is on the right posterior tympanum
	RW4 (10.97%)	The variation is characterized by the constriction right posterior tympanum. While the expansion is on the left tympanum and anterior to left and right midpoint of right tympanum	The variation is characterized by the constriction left tympanum and anterior to left and right midpoint of right tympanum. While the expansion is on the right posterior tympanum
	RW5 (7.50%)	The variation is characterized by the constriction right posterior tympanum. While the expansion is on the left tympanum and anterior to left and right midpoint of right tympanum	The variation is characterized by the constriction right posterior tympanum. While the expansion is on the left tympanum

Table 3. Summary of the MANOVA results

Trait	Wilks´ lambda	Pillai trace	F (df_1, df_2)	p-value	Effect size (η^2)
Head Shape	0.416	0.584	26.17 (3, 56)	**1.034E-10**	0.584
Snout Shape	0.619	0.381	8.45 (4, 55)	**2.177E-05**	0.381
Tympanum Shape	0.632	0.368	6.28 (5, 54)	**0.0001159**	0.368

Note: Bold: Significant

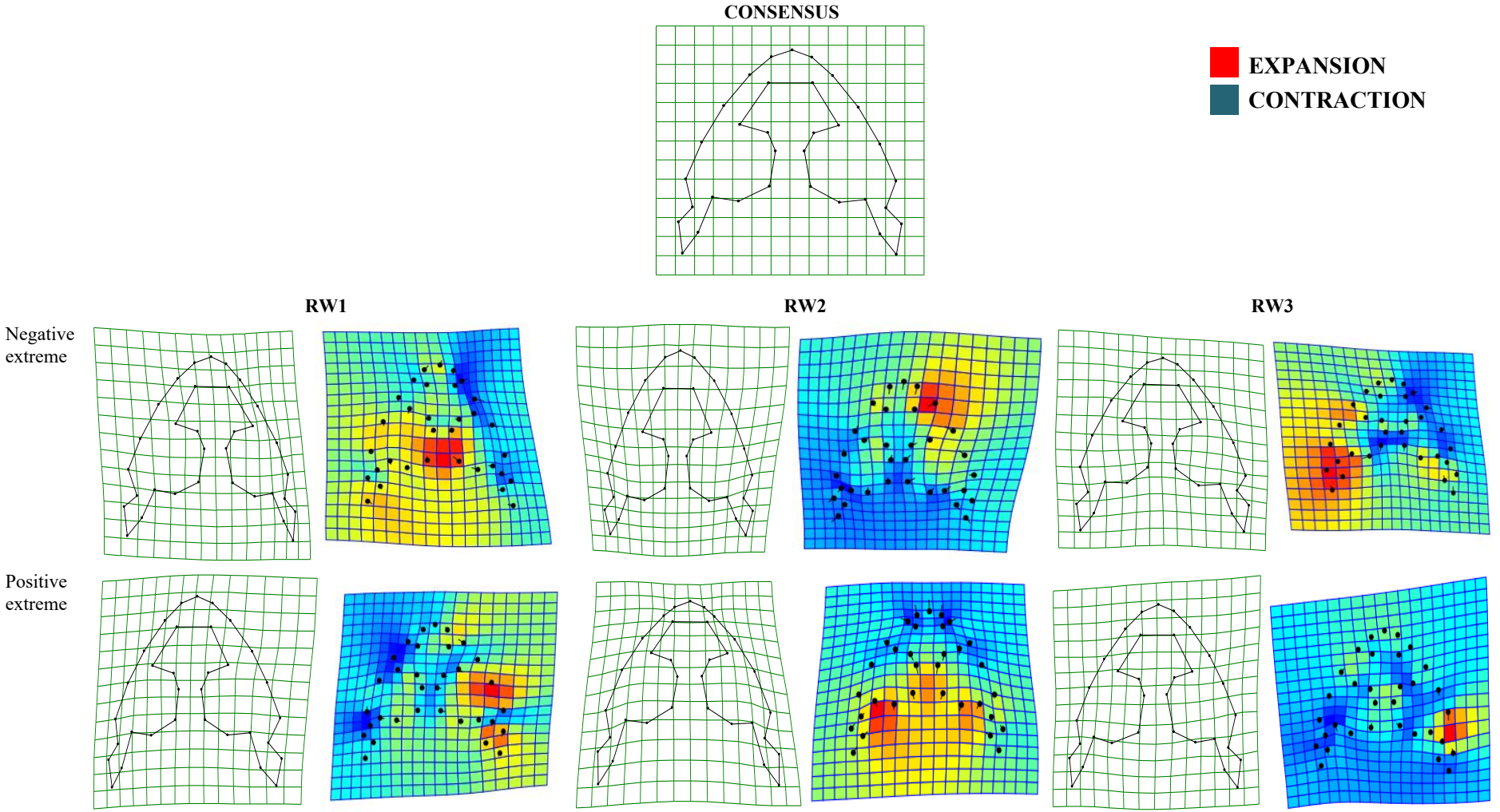

Figure 5. Significant relative warps and heat map of the head shape of *Hoplobatrachus rugulosus*

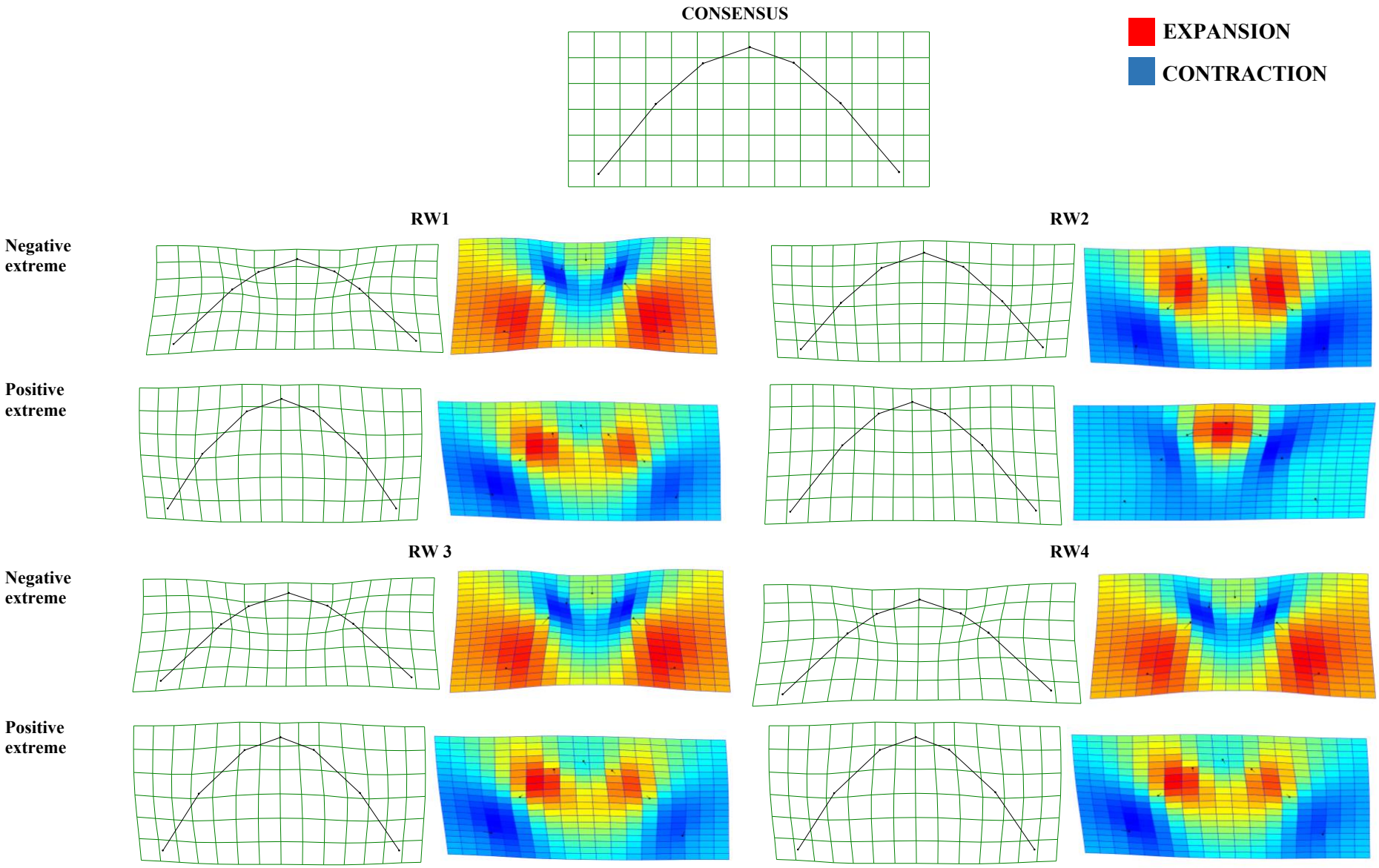

Figure 6. Significant relative warps and heat map of the snout shape of *Hoplobatrachus rugulosus*

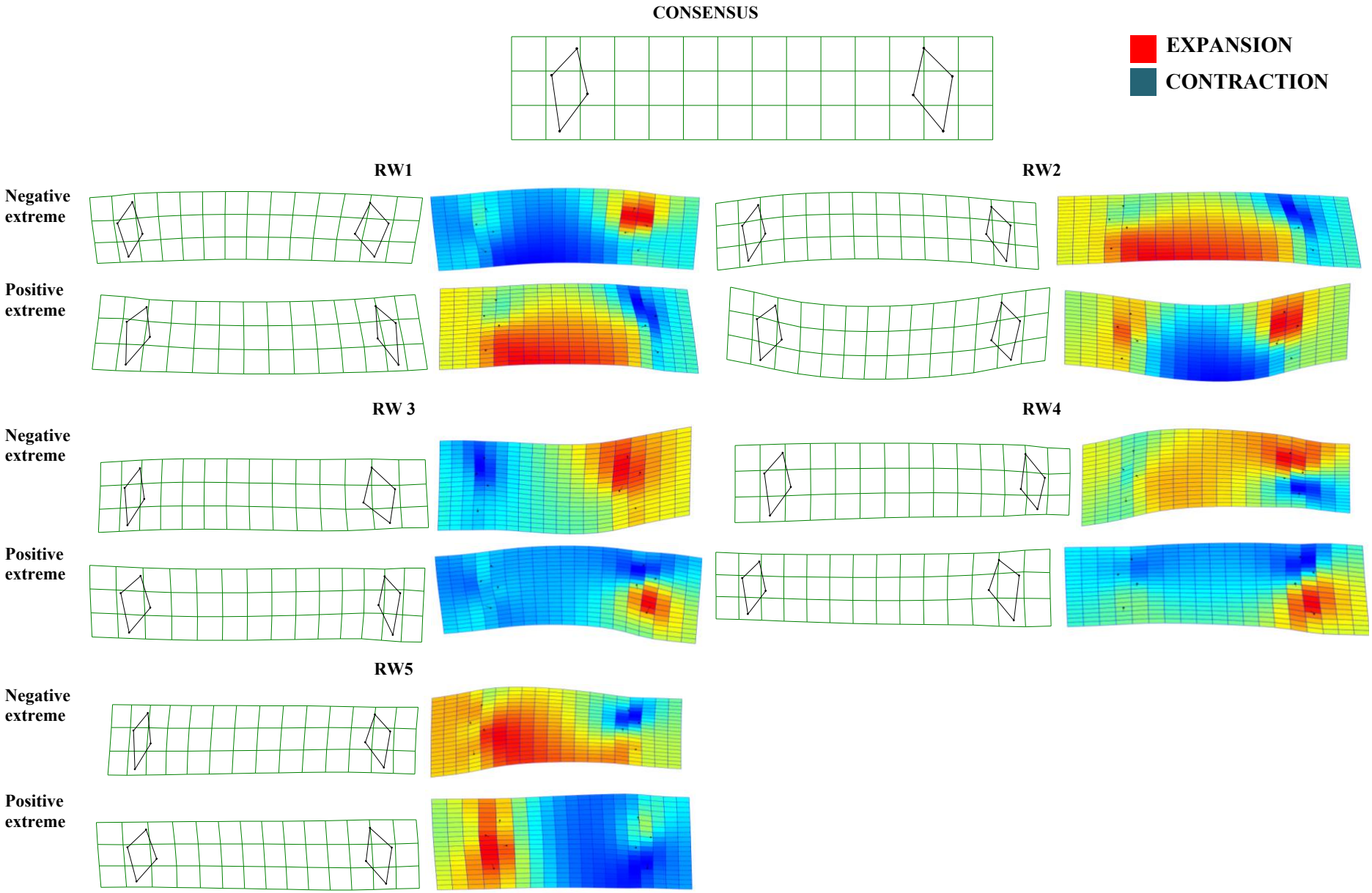

Figure 7. Significant relative warps and heat maps of the tympanum shape of *Hoplobatrachus rugulosus*

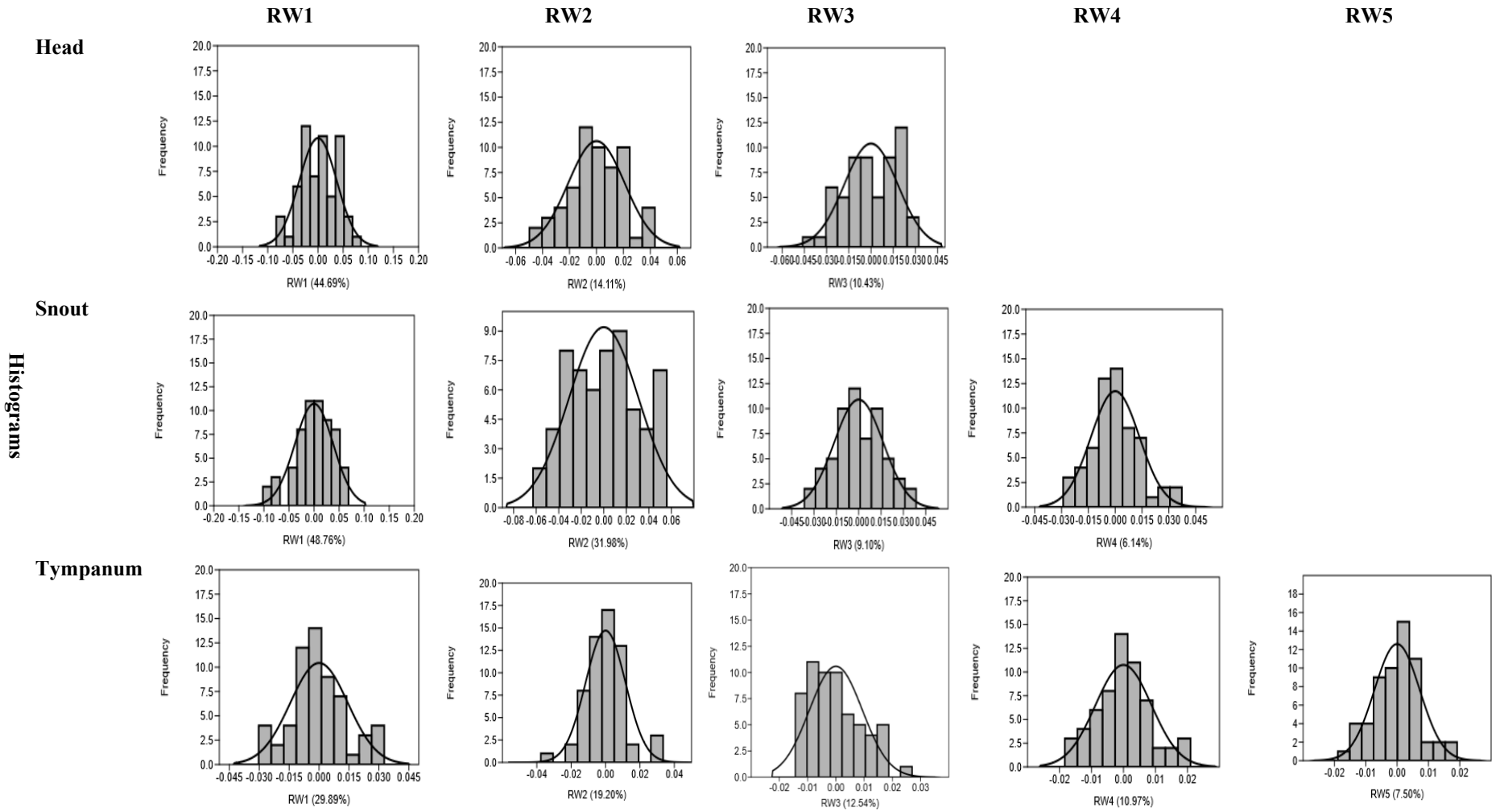

Figure 8. Histogram of the significant relative warps of the head, snout and tympanum shapes of *Hoplobatrachus rugulosus*

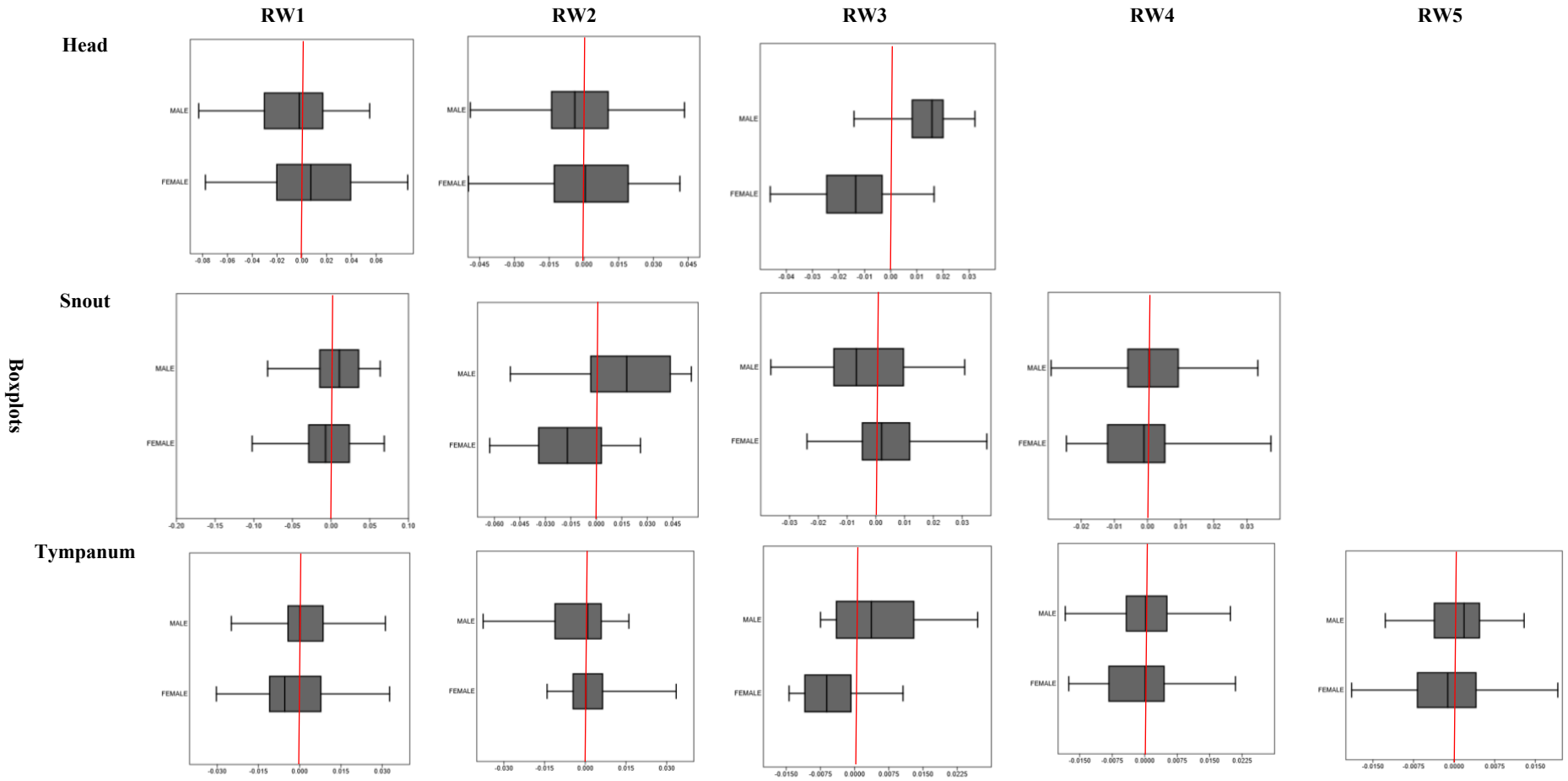

Figure 9. Boxplots of the significant relative warps of the head, snout and tympanum shapes of *Hoplobatrachus rugulosus*

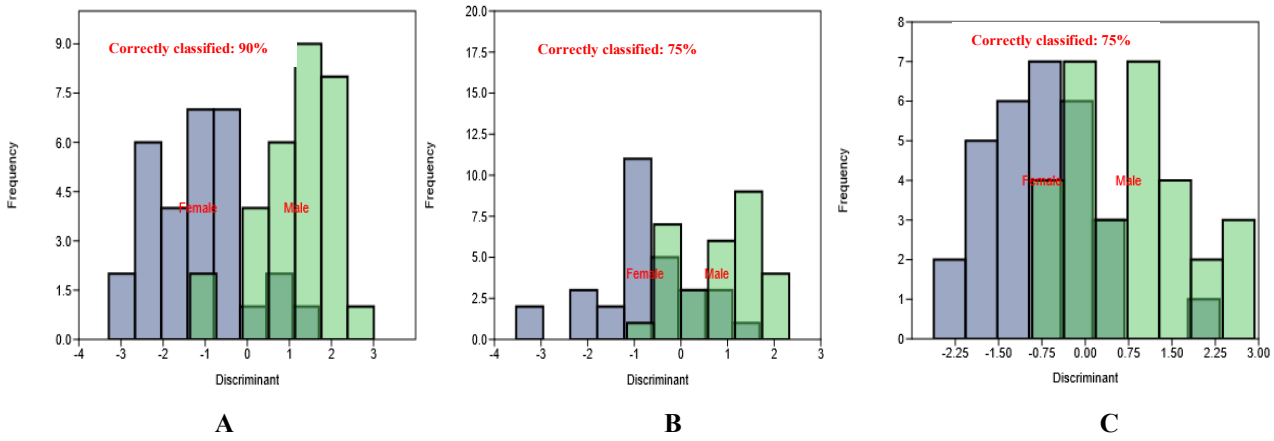

Figure 10. Discriminant function analysis of: A. Head, B. Snout, and C. Tympanum shapes of *Hoplobatrachus rugulosus*

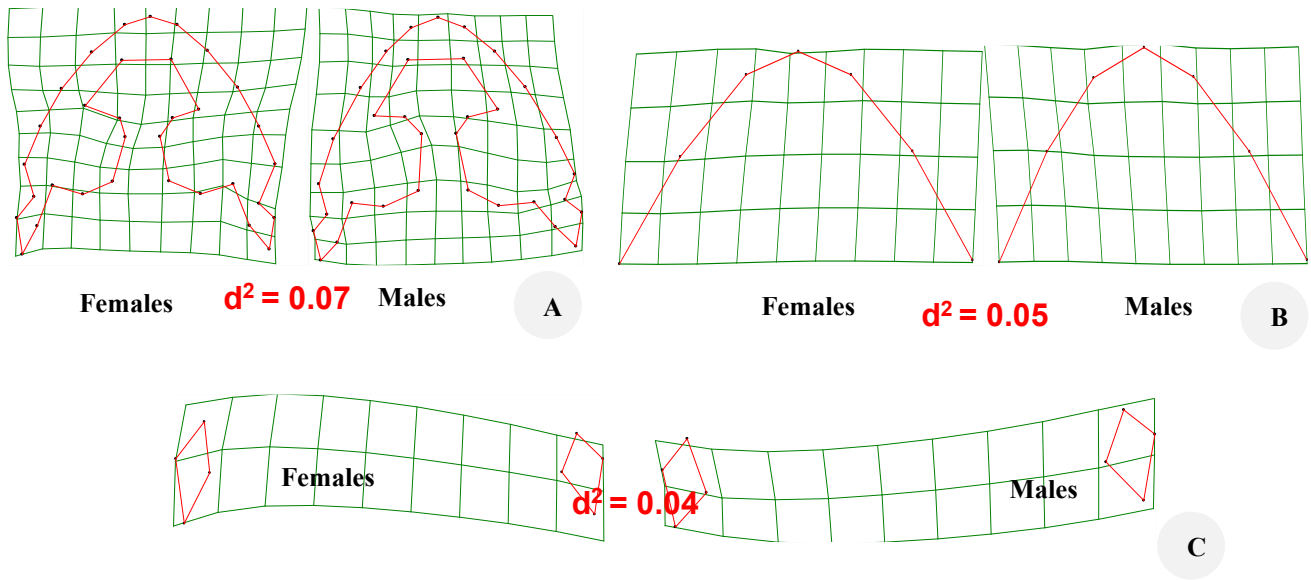

Figure 11. Procrustes distance of the: A. Head, B. Snout, and C. Tympanum shapes of female and male *Hoplobatrachus rugulosus*

Table 5. Summary of sexual dimorphism in head, snout, and tympanum shape

Morphological trait	Sex	Key shape characteristics	Functional/ecological implication
Head shape	Female	Narrower snout, broader jaw, tympanum, and eye region	Reflects fecundity selection; larger, more even heads linked to egg-carrying and feeding
	Male	Expanded snout, jaw, and eye areas with localized narrowing	Linked to reproductive behaviors: calling, burrowing, or territorial defense
Snout shape	Female	Anterior and mid-snouts narrower; posterior maxilla broader (symmetrical)	Suggests adaptation for capturing larger prey; reflects ecological role and reproductive investment
	Male	Alternates between wider snouts or jaws	May indicate individual variation in reproductive tactics or foraging strategy
Tympanum shape	Female	Constriction in right posterior and expansion in anterior and left regions	Reflects reduced auditory demands; greater morphological tolerance
	Male	Constriction either left or right with anterior narrowing; expansions in specific regions	Related to acoustic communication, mate attraction, and heightened auditory sensitivity

Table 4. The value of head parameters of *Hoplobatrachus rugulosus*

	Males (n = 30) Mean±SD	Females (n = 30) Mean±SD	p-value (<0.05)
Snout-vent length (mm)	98.55±3.07	117.62±2.55	**7.90994E-34**
Head length (mm)	28.89±2.16	29.54±2.29	**0.001165054**
Head breath (mm)	31.33±2.07	33.26±2.84	0.324885284

Note: Bold: Significant

Discussion

Head shape variation

Males and females of *H. rugulosus* exhibited distinct patterns in head shape based on relative warp analysis. In males, shape changes appeared more uneven and spread out, with narrowing primarily on the right front part of the head and widening in areas such as the snout, jaw, and around the eyes. These changes occurred on both sides and in various parts of the head, resulting in a more asymmetrical appearance. In contrast, females have a more balanced shape and follow a more precise pattern. The front part of the head, especially the snout, is usually narrower, while the back part, around the jaw, tympanum, and eyes, is wider. Overall, male head shapes are more irregular, while female head shapes are more even and follow a narrow-front to wide-back pattern.

The results indicated that females generally had wider head shapes than males. This may reflect female-biased size dimorphism, a widespread pattern in anurans where 90% of female species tend to be larger than males (Bell and Zamudio 2012). In rusty toads *Rhinella rubescens*, for instance, da C Arantes et al. (2015) reported wider heads in females. Such patterns are often attributed to fecundity selection, where larger female body size enhances reproductive capacity (Shine 1979; Bell and Zamudio 2012; Nali et al. 2014). Moreover, Monnet et al (2002) and Liao et al. (2013) highlight that size differences between male and female anurans are primarily influenced by age-related growth and reproductive timing (Traijitt 2020). Females tend to reproduce later, grow more slowly, and live longer, allowing for extended development. These factors may also explain the broader head dimensions observed in female *H. rugulosus*. Additionally, females consistently exhibit a wider Inter-Quartile Range (IQR) across all three RWs, suggesting greater variation in head shape compared to males. According to Schäuble (2004), the greater shape variation observed in females might reflect adaptive flexibility for varied ecological roles.

In this study, male *H. rugulosus* exhibited more irregular head shapes, which could be associated with behaviors such as vocalization and intrasexual competition, although no behavioral data were collected to confirm this. These behaviors likely impose selective pressures on cranial morphology, contributing to the development of more specialized or asymmetric head features that support reproductive success (Goyes Vallejos et al. 2021). Previous studies suggest that cranial morphology in anurans can be influenced by sexual selection, particularly in species where males compete for mates (Goyes Vallejos et al. 2021). Among other Dicroglossidae species, *Rana kuhlii*, males have been reported to possess relatively larger head sizes than females (Tsuji and Matsui 2001), supporting Shine's (1979) hypothesis that sexually dimorphic traits such as enlarged heads or jaws in male anurans are adaptations linked to intrasexual competition and sexual selection. During the mating season, males compete for access to females, with larger individuals often being more successful in physical confrontations (Emerson 2000). In contrast, medium- or smaller-sized males may rely on speed and agility to reach females quickly (Goyes Vallejos et al. 2021). Therefore, the observed sexual dimorphism in *H. rugulosus* appears to result from a combination of fecundity-driven natural selection, vocalization and sexual selection through intrasexual aggression (Nali et al. 2014; de Abreu e Melo-Moreira et al. 2021), however, without functional or behavioral validation in *H. rugulosus*, these interpretations remain speculative.

Snout shape variation

In the study, females exhibited a clear and consistent snout morphology, marked by constriction in the anterior and mid-snout regions and expansion in the posterior maxilla. This pattern reflects a general narrowing at the front and widening toward the back of the snout, resulting in a more rounded and shorter snout. Some male *H. rugulosus* exhibited more pointed snouts and narrower jaws, while others displayed the opposite configuration. These alternating patterns suggest dynamic cranial variability among males, potentially reflecting diverse functional roles or reproductive strategies (Schäuble 2004). This contrasts with females, whose snout morphology appeared more consistent and directionally shaped, indicating greater morphological stability (Fondren 2023).

Similar findings were reported by Fondren (2023), who observed that female *A. americanus* exhibited rounder and more uniform rostral shapes compared to phenotypic males. The observed differences in snout shape may reflect niche partitioning of food resources between sexes. Moreover, Donol et al (2025) found that snout morphology is closely linked to feeding behavior, with wider snouts enabling access to a broader range of prey. As noted by Crnobrnja-Isailović et al. (2012), larger-bodied females may not consume a broader range of prey types taxonomically, but their size enables them to exploit a wider size spectrum of available prey. This physiological advantage may not alter dietary diversity but could enhance feeding flexibility by allowing access to larger prey items. This trait can be particularly advantageous in habitats with high interspecific competition or elevated predation pressure, allowing individuals to exploit varied food sources more efficiently.

However, the findings of Lin and Ji (2005) present a contrasting perspective. While they acknowledged a general association between head size and diet, their study revealed that both sexes of *H. rugulosus* consumed largely similar types of food, with substantial overlap in food niches. Their study suggests that the slight sexual dimorphism in head or snout morphology does not play a significant role in dietary separation. Moreover, potential dietary

differences between sexes did not appear to directly influence changes in head size during development or contribute to the emergence of sexual dimorphism. Thus, their findings suggest that snout shape differences may not be primarily driven by ecological factors such as resource partitioning.

The differences between our findings and those of Lin and Ji (2005) may stem from variations in population, season, and methodology. Their study used gut content analysis and reported dietary overlap, while our geometric morphometric approach reveals potential functional differences in morphology rather than direct feeding behavior. Moreover, our specimens were collected over a short 19-day period from March to April, just before peak breeding season, where ecological pressures such as prey diversity and environmental stressors may intensify selective pressures on snout shape.

Thus, while our findings suggest potential functional roles for snout morphology possibly linked to feeding efficiency or reproductive adaptation (Indermaur et al. 2010; Womack and Bell 2020; Sapkota et al. 2022), these interpretations remain hypotheses without direct behavioral or dietary validation. It is also possible that selection on snout shape arises from multiple interacting factors, including habitat structure and reproductive roles, rather than solely from trophic divergence (Indermaur et al. 2010; Sapkota et al. 2022; Goldberg et al. 2024).

Tympanum shape variation

The study revealed differences in tympanum shape in *H. rugulosus*, which may indicate functionally and evolutionarily significant dimorphism. Specifically, females generally exhibited constriction on the right posterior portion of the tympanum, with expansion occurring on the left tympanum and the anterior region leading to the left and right midpoints of the right tympanum. In contrast, males showed a distinct pattern characterized by constriction on either the right or left tympanum, with the anterior region approaching the midpoint of the right tympanum. Tympanic expansion in males was typically observed on the left tympanum or the right posterior tympanum. Interestingly, results of the study showed that both male and female *H. rugulosus* exhibited Fluctuating Asymmetry (FA) in tympanum shape. As defined by Bosch and Márquez (2000), FA refers to small, random deviations from perfect bilateral symmetry in paired structures, such as the left and right tympana, that are expected to be identical under normal developmental conditions.

Fluctuating Asymmetry (FA) is a recognized indicator of developmental instability caused by genetic or environmental stress and may affect key functions such as sound localization in anuran (Bosch and Márquez 2000). In this study, FA was consistently observed in both sexes of *H. rugulosus*, suggesting exposure to stress during development (Gallant and Teather 2001; Zakharov and Trofimov 2022). Likely sources of stress include agrochemical contamination from rice paddies, which can disrupt endocrine and developmental processes (Benderlioglu 2010), and chronic noise pollution from agricultural activity (Zhelev et al. 2023). Additionally, habitat alteration due to land-use intensification may contribute to developmental instability (Bee and Swanson 2007; Zhelev et al. 2023). Although environmental variables were not directly assessed, the consistent presence of FA indicates a possible link to anthropogenic disturbance and reduced habitat quality.

Moreover, the presence of FA in both sexes could suggest subtle developmental disturbances that could affect auditory performance and reproductive success. As noted by Tonini et al. (2020), tympanum shape in frogs is closely associated with sound perception and mating behavior. Supporting this, Wang et al. (2016) found that male Chinese tiger frogs (*H. rugulosus*) have a larger tympanic membrane surface area than females, suggesting that different tympanic dimensions may evolve independently to meet sex-specific acoustic demands. Males are likely under stronger selective pressures for enhanced auditory sensitivity due to their role in producing and responding to calls during mate competition in the breeding season (James et al. 2022; Tonini et al. 2020). Accurately distinguishing conspecific vocal signals from environmental noise is particularly important during this period (Bosch and Márquez 2000; Wang et al. 2016). These acoustic and ecological pressures could have contributed to the evolution of sexually dimorphic traits through sexual selection, often leading to the exaggeration of certain body proportions in males, such as the tympanum.

In many anuran species, males possess relatively larger tympana, which may improve their ability to detect and respond to mating calls (Hetherington 1992; Tonini et al. 2020). Since females typically select mates based on call frequency, selection may favor males with tympanic structures optimized for both sound production and perception (Gerhardt 1994; Gerhardt and Bee 2007). In contrast, females, who do not produce advertisement calls, rely primarily on auditory sensitivity for locating potential mates (James et al. 2022). These intersexual differences in tympanic membrane structure and shape likely may represent divergent evolutionary responses to reproductive and environmental pressures. Thus, while sex appears to influence tympanum shape variation, reproductive strategy, sexual selection, and habitat-related acoustic challenges also contribute to the morphological diversity observed in this trait.

This study revealed significant sexual dimorphism in *H. rugulosus*, particularly in head, snout, and tympanum shape. Females exhibited wider and more symmetrical cranial features, supporting fecundity-related roles such as egg production and feeding flexibility. In contrast, males displayed more irregular and asymmetrical shapes, especially in the snout and tympanum, likely reflecting adaptations for acoustic signaling and mate competition. The presence of fluctuating asymmetry in tympanum shape across both sexes suggests subtle developmental stress, potentially linked to environmental factors. Geometric morphometrics proved valuable in detecting subtle, functionally relevant shape differences that traditional linear measurements may overlook. However, this method requires standardized imaging, technical expertise, and specialized software, which may limit its accessibility and

application in field settings. Future research should integrate additional traits particularly bite force, which may be closely linked to head shape variation and feeding performance. Moreover, investigating mating acoustics can provide insight into the behavioral relevance of cranial dimorphism. Moreover, biomechanical and behavioral parameters could also offer a more comprehensive understanding of sexual dimorphism in this species and its potential ecological or evolutionary drivers.

ACKNOWLEDGEMENTS

The author extends heartfelt gratitude to Prof. Muhmin Micahel E. Manting and Prof. Kimverly Hazel C. Dapar for their dedicated guidance in geometric morphometrics. Special thanks are also extended to Khean Harvey Acuevas, Adrian Aturo, Ellaiza Tigbabao, and Hazelle Rizalda for their valuable assistance during the conduct of the study. Lastly, the author also gratefully acknowledges the Department of Science and Technology-Science Education Institute (DOST-SEI) through the STRAND Scholarship Program for scholarship support.

REFERENCES

Bee MA, Swanson EM. 2007. Auditory masking of anuran advertisement calls by road traffic noise. Anim Behav 74 (6): 1765-1776. DOI: 10.1016/j.anbehav.2007.03.019.

Bell RC, Zamudio KR. 2012. Sexual dichromatism in frogs: Natural selection, sexual selection and unexpected diversity. Proc Biol Sci 279 (1748): 4687-4693. DOI: 10.1098/rspb.2012.1609.

Benderlioglu Z. 2010. Fluctuating asymmetry and steroid hormones: A review. Symmetry 2 (2): 541-553. DOI: 10.3390/sym2020541.

Bosch J, Márquez R. 2000. Tympanum fluctuating asymmetry, body size and mate choice in female midwife toads (*Alytes obstetricans*). Behaviour 137: 1211-1222. DOI: 10.1163/156853900502600.

Cabuga Jr CC, Empeño AMD, Pondang JMD. 2025. Geometric morphometric analysis of body shape variation in *Glossogobius giuris* from Lake Mainit, Agusan del Norte, Philippines. Res Ecol 7 (2): 144-158. DOI: 10.30564/re.v7i2.9519.

Caldart VM, Loebens L, Brum AJC, Bataioli L, Cechin SZ. 2019. Reproductive cycle, size and age at sexual maturity, and sexual dimorphism in the stream-breeding frog *Crossodactylus schmidti* (Hylodidae). S Am J Herpetol 14 (1): 1-11. DOI: 10.2994/sajh-d-17-00060.1.

Chen H, Qin H, Zhao Z, Liao J, Wu Y, Liu X, Jiang L, Dayanda B, Chen W. 2023. Body size but not food size determined head sexual dimorphism in *Rana kukunoris* from the Tibetan Plateau. Asian Herpetol Res 14: 175-181. DOI: 10.3724/ahr.2095-0357.2022.0060.

Crnobrnja-Isailović J, Ćurčić S, Stojadinović D, Tomašević-Kolarov N, Aleksić I, Tomanović Ž. 2012. Diet composition and food preferences in adult common toads (*Bufo bufo*) (Amphibia: Anura: Bufonidae). J Herpetol 46 (4): 562-567. DOI: 10.1670/10-264.

Da C Arantes Í, Vasconcellos MM, Boas TCV, Veludo LBA, Colli GR. 2015. Sexual dimorphism, growth, and longevity of two toad species (Anura, Bufonidae) in a Neotropical Savanna. Copeia 103 (2): 329-342. DOI: 10.1643/CH-14-092.

Dapar MLG, Garcia SMG, Achacoso MVD, Debalucos CAP, Moneva CSO, Demayo CG. 2014. Describing populations of *Pomacea canaliculata* Lamarck from selected areas in Mindanao, Philippines using relative warp analysis of the whorl shell shape. Aust J Basic Appl Sci 8 (5): 355-360.

Dapar MLG, Manting MME, Sasan LG, Arimao RGG, Demayo CG. 2015. Correlation of measured intelligence and facial morphology among the selected students of Mindanao State University-Iligan Institute of Technology, Iligan City, Philippines. Adv Environ Biol 9 (19): 41-49.

de Abreu e Melo-Moreira D, Murta-Fonseca RA, Galdino CAB, Nascimento LB. 2021. Does a male nest builder have the same head shape as his mate? Sexual dimorphism in *Leptodactylus fuscus* (Anura: Leptodactylidae). Zool Anz 295: 23-33. DOI: 10.1016/j.jcz.2021.09.004.

Delima EMM, Ates FB, Ibañez JC. 2006. Species composition and microhabitats of frogs within Arakan Valley Conservation Area, Cotabato, Mindanao Island, Philippines. Banwa 3: 16-30

Diesmos AC, Diesmos ML, Brown RM 2008. Status and distribution of alien invasive frogs in the Philippines. J Environ Sci Manag 9 (2): 41-53.

Donol CM, Zainudin R, Deka EQ. 2025. Morphological variation of *Pelobatrachus nasutus* (Schlegel, 1858) (Order: Anura and Family: Dicroglosidae) from different localities in Sarawak. J Sustain Sci Manag 20 (2): 390-406. DOI: 10.46754/jssm.2025.02.013.

Emerson SB. 2000. Vertebrate secondary sexual characteristics—Physiological mechanisms and evolutionary patterns. Am Nat 156 (1): 84-91. DOI: 10.1086/303370.

Flores GMA, Torres AG, Flores ABA, Jakosalem PGC, Guihawan JQ, Roa-Quiaoit HA. 2024. Species composition and conservation of amphibians in Central Panay Mountain Range, Antique, Philippines. Biodiversitas 25 (4): 1797-1808. DOI: 10.13057/biodiv/d250450.

Fondren A. 2023. Variation and sexual dimorphism in color and head morphology in American toads (*Anaxyrus americanus*). [Thesis]. Saint Cloud State University, USA.

Gallant N, Teather K. 2001. Differences in size, pigmentation, and fluctuating asymmetry in stressed and nonstressed northern leopard frogs (*Rana pipiens*). Écoscience 8 (4): 430-436. DOI: 10.1080/11956860.2001.11682671.

Gerhardt HC, Bee MA. 2007. Recognition and localization of acoustic signals. In: Narins PM, Feng AS, Fay RR, Popper AN (eds). Hearing and Sound Communication in Amphibians. Springer, New York. DOI: 10.1007/978-0-387-47796-1_5.

Gerhardt HC. 1994. The evolution of vocalization in frogs and toads. Ann Rev Ecol Syst 25: 293-324. DOI: 10.1146/annurev.es.25.110194.001453.

Goldberg J, Naretto S, Carezzano F, Quinzio S. 2024. Sexual size dimorphism in multiple traits: An integrative perspective in several Anuran species. J Herpetol 58 (1): 46-63. DOI: 10.1670/22-079.

Goyes Vallejos J, Gomez J, Hernández-Figueroa AD, Vera R. Green DM. 2021. Fertilization success suggests random pairing in frogs with regard to body size. Behav Ecol Sociobiol 75 (10): 140. DOI: 10.1007/s00265-021-03081-6.

Hammer Ø, Harper DAT, Ryan PD. 2001. PAST: Paleontological Statistics software package for education and data analysis. Palaeontol Electron 4 (1): 1-9.

Haribon Foundation. 2004. Guidelines for Amphibians and Reptiles Survey. Haribon Foundation.

Hetherington TE. 1992. The effects of body size on the functional properties of middle ear systems in anuran amphibians. Brain Behav Evol 39 (3): 133-142. DOI: 10.1159/000114111.

Ilić M, Jojic V, Stamenković G, Marković V, Simic VM, Paunović M, Crnobrnja-Isailovic J. 2019. Geometric vs. traditional morphometric methods for exploring morphological variation of tadpoles at early developmental stages. Amphibia-Reptilia 40 (4): 1-11. DOI: 10.1163/15685381-00001193.

Indermaur L, Schmidt BR, Tockner K, Schaub M. 2010. Spatial variation in abiotic and biotic factors in a floodplain determine anuran body size and growth rate at metamorphosis. Oecologia 163 (3): 637-649. DOI: 10.1007/s00442-010-1586-4.

James LS, Taylor RC, Hunter KL, Ryan MJ. 2022. Evolutionary and allometric insights into anuran auditory sensitivity and morphology. Brain Behav Evol 97 (3-4): 140-150. DOI: 10.1159/000521309.

Juarez BH, Moen DS, Adams DC. 2023. Ecology, sexual dimorphism, and jumping evolution in anurans. J Evol Biol 36 (5): 829-841. DOI: 10.1111/jeb.14171.

Kaliontzopoulou A. 2011. Geometric morphometrics in herpetology: Modern tools for enhancing the study of morphological variation in amphibians and reptiles. Basic Appl Herpetol 25: 5-32. DOI: 10.11160/bah.11016.

Liao WB, Zeng Y, Yang JD. 2013. Sexual size dimorphism in anurans: Roles of mating system and habitat types. Front Zool 10 (1): 65. DOI: 10.1186/1742-9994-10-65.

Lin Z, Hong Y, Chen S, Zhang Q, Han L, Tu W, Du Y, Gu S, Yuan Z, Hu S, Liu X. 2023. Emerging non-native amphibians require immediate prevention management in a megacity of South China. BioInvasions Rec 12 (3): 731-744.

Lin Z-H, Ji X. 2005. Sexual dimorphism in morphological traits and food habits in tiger frogs, *Hoplobatrachus rugulosus*, in Lishui, Zhejiang. Zool Res 26 (3): 255-262.

Monnet J-M, Cherry MI. 2002. Sexual size dimorphism in anurans. Proc Biol Sci 269 (1507): 2301-2307. DOI: 10.1098/rspb.2002.2170.

Murta-Fonseca RA, Folly M, Carmo LF, Martins A. 2020. Growing towards disparity: Geometric morphometrics reveals sexual and allometric differences in *Aparasphenodon brunoi* (Anura: Hylidae: Lophyohylinae) head shape. Cuad Herpetol 34 (1): 1-11. DOI: 10.31017/CdH.2020.(2019-032).

Nali RC, Zamudio KR, Haddad CFB, Prado CPA. 2014. Size-dependent selective mechanisms on males and females and the evolution of sexual size dimorphism in frogs. Am Nat 184 (6): 727-740. DOI: 10.1086/678455.

Nuñeza OM, Non MLP, Oconer EP, Aljibe MC. 2017. Species richness and endemism of anurans in Mt. Matutum protected landscape, South Cotabato, Philippines. J Biodivers Environ Sci 10 (5): 1-13.

Petrović TG, Vukov TD, Kolarov NT. 2017. Sexual dimorphism in size and shape of traits related to locomotion in nine anuran species from Serbia and Montenegro. Folia Zool 66 (1): 11-21. DOI: 10.25225/fozo.v66.i1.a4.2017.

Pincheira-Donoso D, Harvey LP, Grattarola F, Jara M, Cotter SC, Tregenza T, Hodgson DJ. 2021. The multiple origins of sexual size dimorphism in global amphibians. Glob Ecol Biogeogr 30 (2): 443-458. DOI: 10.1111/geb.13230.

Portik DM, Bell, RC, Blackburn DC et al. 2019. Sexual dichromatism drives diversification within a major radiation of African amphibians. Syst Biol 68 (6): 859-875. DOI: 10.1093/sysbio/syz023.

Račković JK, Kolarov NT, Vukov T. 2019. The ventral cranial size and shape variation between males and females of European brown frogs: *Rana dalmatina, R. graeca* and *R. temporaria* (Anura, Amphibia). Nat Sci 9 (2): 6-11. DOI: 10.5937/univtho9-21223.

Rongchapho P, Thongproh P, Chuaynkern C, Intuman C, Chuaynkern Y. 2021. Clutch size of the Rugose Frog, *Hoplobatrachus rugulosus* (Wiegmann, 1834), from Phu Khiao Wildlife Sanctuary, Northeastern Thailand. Herpetol Notes 14: 1253-1256.

Sapkota S, Bhattarai BP, Mishra MR, Adhikari JN, Khatiwada JR. 2022. Diet composition and overlap of sympatric amphibians in paddy fields of Nepal. Herpetol Conserv Biol 17 (1): 155-164.

Schäuble CS. 2004. Variation in body size and sexual dimorphism across geographical and environmental space in the frogs *Limnodynastes tasmaniensis* and *L. peronii.* Biol J Linn Soc 82 (1): 39-56. DOI: 10.1111/j.1095-8312.2004.00315.x.

Shine R. 1979. Sexual selection and sexual dimorphism in the Amphibia. Copeia 1979 (2): 297-306. DOI: 10.2307/1443418.

Silva NR, Berneck BVM, da Silva HR, Haddad CFB, Zamudio KR, Mott T, Nali RC, Prado CPA. 2020. Egg-laying site, fecundity and degree of sexual size dimorphism in frogs. Biol J Linn Soc 131 (3): 600-610. DOI: 10.1093/biolinnean/blaa126.

Solania CL, Fernandez-Gamalinda EV. 2018. Species composition and habitat association of anurans within water systems of Andanan Watershed, Agusan del Sur, Caraga Region, Philippines. Environ Exp Biol 16: 159-168. DOI: 10.22364/eeb.16.15.

Solis MF, Arroyo Jr J, Garcia KA, Zapico F, Requieron E. 2015. Geometric morphometric analysis on sexual dimorphism of guppy *Poecilia reticulata* in Lake Sebu, South Cotabato, Philippines. Res J Anim Vet Fish Sci 3 (1): 1-9.

Tokita M, Iizuka J, Eto K. 2023. Characterization of the adaptive morphology of the stream brown frog, *Rana sakuraii* Matsui & Matsui, 1990, using geometric morphometrics. Herpetol Notes 16: 761-771.

Tonini JFR, Provete DB, Maciel NM, Morais AR, Goutte S, Toledo LF, Pyron RA. 2020. Allometric escape from acoustic constraints is rare for frog calls. Ecol Evol 10 (8): 3686-3695. DOI: 10.1002/ece3.6155.

Traijitt T. 2020. Gonadal sex differentiation of rice field frog *Hoplobatrachus rugulosus* (Wiegmann, 1834). [Dissertation]. Chulalongkorn University, Bangkok, Thailand. DOI: 10.58837/chula.the.2020.24.

Tsuji H, Matsui M. 2002. Male-male combat and head morphology in a fanged frog (*Rana kuhlii*) from Taiwan. J Herpetol 36 (3): 520-526. DOI: 10.1670/0022-1511(2002)036[0520:MMCAHM]2.0.CO;2.

Üzüm N, Özdemir N, Dursun C, Kutrup B, Gül S. 2021. Interspecific and intraspecific size and shape variation in skull of two closely related species, *Bufo bufo* (Linnaeus, 1758) and *Bufo verrucosissimus* (Pallas, 1814) from Turkey. Turk J Zool 45 (2): 91-101. DOI: 10.3906/zoo-2009-8.

Vági B, Végvári Z, Liker A, Freckleton RP, Székely T. 2020. Climate and mating systems as drivers of global diversity of parental care in frogs. Glob Ecol Biogeogr 29 (8): 1373-1386. DOI: 10.1111/geb.13113.

Wang JC, Wang TL, Fu SH, Brauth SE, Cui JG. 2016. Auditory brainstem responses in the Chinese tiger frog *Hoplobatrachus chinensis* (Osbeck, 1765) (Anura: Dicroglossidae) reveal sexually dimorphic hearing sensitivity. Ital J Zool 83 (4): 482-489. DOI: 10.1080/11250003.2016.1222638.

Wei L, Shao W, Ding G, Fan X, Lin Z. 2014. Density but not kinship regulates the growth and developmental traits of Chinese tiger frog (*Hoplobatrachus chinensis*) tadpoles. Asian Herpetol Res 5: 113-118.

Womack MC, Bell RC. 2020. Two-hundred million years of anuran body-size evolution in relation to geography, ecology and life history. J Evol Biol 33 (10): 1417-1432. DOI: 10.1111/jeb.13679.

Yang YJ, Jiang Y, Mi ZP, Liao WB. 2022. Testing the role of environmental harshness and sexual selection in limb muscle mass in anurans. Front Ecol Evol 10: 879885. DOI: 10.3389/fevo.2022.879885.

Zakharov VM, Trofimov IE. 2022. Fluctuating asymmetry as an indicator of stress. Emerg Top Life Sci 6: 295-301. DOI: 10.1042/etls20210274.

Zhelev Z, Mollov I, Tsonev S. 2023. Application of fluctuating asymmetry values in *Pelophylax ridibundus* (Amphibia: Anura: Ranidae) meristic traits as a method for assessing environmental quality of areas with different degrees of urbanization. Diversity 15 (1): 118. DOI: 10.3390/d15010118.